*fractal and fractional*

MDPI

*Article*

# Damage Law and Reasonable Width of Coal Pillar under Gully Area: Linking Fractal Characteristics of Coal Pillar Fractures to Their Stability

**Zhaopeng Wu [1,2], Yunpei Liang [1,2,*], Kaijun Miao [3,*], Qigang Li [1,2], Sichen Liu [1,2], Qican Ran [1,2], Wanjie Sun [1,2], Hualong Yin [4] and Yun Ma [4]**

[1] State Key Laboratory of Coal Mine Disaster Dynamics and Control, Chongqing University, Chongqing 400044, China; zhaopengwu@cqu.edu.cn (Z.W.)
[2] School of Resources and Safety Engineering, Chongqing University, Chongqing 400044, China
[3] State Key Laboratory for Fine Exploration and Intelligent Development of Coal Resources, School of Mines, China University of Mining and Technology, Xuzhou 221116, China
[4] Sunjiacha Longhua Mining Co., Ltd., Shaanxi Coal Chemical Industry Group, Yulin 719314, China
* Correspondence: liangyunpei@cqu.edu.cn (Y.L.); 01140149@cumt.edu.cn (K.M.)

**Abstract:** The coal pillar is an important structure to control the stability of the roadway surrounding rock and maintain the safety of underground mining activities. An unreasonable design of the coal pillar size can result in the failure of the surrounding rock structure or waste of coal resources. The northern Shaanxi mining area of China belongs to the shallow buried coal seam mining in the gully area, and the gully topography makes the bearing law of the coal pillar and the development law of the internal fracture more complicated. In this study, based on the geological conditions of the Longhua Mine 20202 working face, a PFC$^{2D}$ numerical model was established to study the damage characteristics of coal pillars under the different overlying strata base load ratios in the gentle terrain area and the different gully slope sections in the gully terrain area, and the coal pillar design strategy based on the fractal characteristics of the fractures was proposed to provide a reference for determining the width of the coal pillars in mines under similar geological conditions. The results show that the reliability of the mathematical equation between the overlying strata base load ratio and the fractal dimension of the fractures in the coal pillar is high, the smaller the overlying strata base load ratio is, the greater the damage degree of the coal pillar is, and the width of the coal pillar of 15 m under the condition of the actual overlying strata base load ratio (1.19) is more reasonable. Compared with the gentle terrain area, the damage degree of the coal pillar in the gully terrain area is larger, in which the fractal dimension of the fracture in the coal pillar located below the gully bottom is the smallest, and the coal pillar in the gully terrain should be set as far as possible to make the coal pillar located below the gully bottom, so as to ensure the stability of the coal pillar.

**Keywords:** coal pillar stability; gully area; base load ratio; fractal characteristics; particle flow code



**Citation:** Wu, Z.; Liang, Y.; Miao, K.; Li, Q.; Liu, S.; Ran, Q.; Sun, W.; Yin, H.; Ma, Y. Damage Law and Reasonable Width of Coal Pillar under Gully Area: Linking Fractal Characteristics of Coal Pillar Fractures to Their Stability. *Fractal Fract.* **2024**, *8*, 407. https://doi.org/10.3390/fractalfract8070407

Academic Editor: Carlo Cattani

Received: 18 June 2024
Revised: 8 July 2024
Accepted: 9 July 2024
Published: 11 July 2024



## 1. Introduction

Located in the gully area of the Loess Plateau, the northern Shaanxi mining area has become one of the world's largest shallow-buried coal seam mines and is an important energy production base in China [1,2]. In underground mining activities, coal pillars are important structures for controlling the stability of roadway surrounding rocks and maintaining the safety of mining operations [3–6]. Due to the shallow burial of coal seams, high mining intensity, and simple overlying strata structure [6], the working face in the northern Shaanxi mining area is more affected by the surface gully topography [7], and the load transfer law of overlying strata and the mine pressure behavior of the working face are more complicated [3,8,9], which bring challenges to the determination of the width of coal pillars when mining shallow buried coal seams in the gully area. A small width

of coal pillar is easy to destabilize and damage, which cannot ensure the safe mining of the working face, while a large width of the coal pillar will cause a large amount of coal resources to be wasted, which is not in line with the development needs of green mining and scientific mining [10].

The width of the coal pillar directly determines the safety of the underground mining space, and several scholars have studied the stability of the coal pillar through theoretical analysis, numerical simulation, and engineering tests [11,12]. Wang Meng et al. [3] obtained the theoretical criterion of the stability of the coal pillar by establishing the models of the overlying stratum structure and the coal pillar stress of the dynamic pressure roadway along the gob, and proposed the reinforcement measures for the coal pillar. The stabilization measures of coal pillars were proposed. Zhang Zhen et al. [6] comprehensively used field testing, theoretical analysis, and numerical simulation to reveal the distribution characteristics and evolution mechanism of the side abutment pressure inside wide coal pillars under the influence of the first mining action, which provides a basis for the strata control of underground mining and wide coal pillar disaster prevention and control. Based on the techniques of microseismic monitoring and moment tensor inversion and velocity tomography, Song Chunhui et al. [13] studied the damage mechanism and stress evolution characteristics of the anomalous zones in the irregular coal pillars, which served as the theoretical basis for analyzing the mechanism of coal pillar damage, destabilization, and induced rock explosion. In addition, other scholars have evaluated the damage degree of coal pillars [14,15]. However, the surface of the northern Shaanxi mining area is mostly a gully terrain [7,16], few scholars have studied the mechanism of the influence of the gully terrain on the stability of coal pillars, and there is no quantitative analysis of the degree of damage to the coal pillars.

At present, most studies on the evolution law of overlying fractures in coal mining use the one-dimensional features of the fissure network to describe the damage range and damage situation of the overlying strata, such as the commonly used development height index of the fissure zone [17]. Due to the existence of natural cracks, joints and bedding, and other weak surfaces in the rock mass, the roof collapses periodically. During the process, the generated fracture network has a scaling effect, which conforms to the characteristics of fractal geometry [18,19]. Therefore, using fractal dimensions is an effective method to characterize the development of fractures and the degree of damage to coal pillars, and has been widely used in mining engineering [5,19,20]. Zhang Gaizhuo et al. [21] quantitatively evaluated the geological structure of coal mines by analyzing the fractal characteristics of fractures. Liu Chao et al. [22] used the fractal method to characterize the fracture evolution process monitored via microseismic technology. However, they are all studied by means of numerical simulation that lacks the fracture function inside the unit, such as FLAC$^{3D}$ and UDEC, which cannot accurately reflect the development and distribution of the fractures, there are very few studies on the use of fractal theory to describe the fractures within the coal pillar, and the influence of the gully topography is not taken into account [23]. In this study, the geological conditions of the 20202 working face in Longhua Coal Mine were used as the engineering background to analyze the stability conditions and design principles of coal pillars when mining shallow buried coal seams in the gully area, a PFC$^{2D}$ particle flow code numerical model was established, and the damage characteristics of coal pillars under different overlying strata base load ratios in the gentle terrain area and different gully slope sections in the gully terrain area were investigated, respectively. The coal pillar design strategy based on the fractal characteristics of fractures was proposed, which can provide a reference for the determination of the width of the coal pillars of the mines under similar geological conditions.

## 2. Engineering Geological Conditions

### *2.1. Study Area and Mining Settings*

Longhua Coal Mine is located in the northern Shaanxi mining area of China. The mine surface is a typical loess gully area, and the 20202 working face is the first mining

face of the 202 panel area of the mine, with an inclination angle of 1° and a burial depth of 124.5~188.5 m. It adopts the method of one-time full-height mining of the thick seams, and manages the roof using the all collapsed method. The 20202 working face is a large mining height working face, and the thickness of the $2^{-2}$ coal seam mined is 6.25~7.39 m, with an average of 6.5 m, as shown in Figure 1.

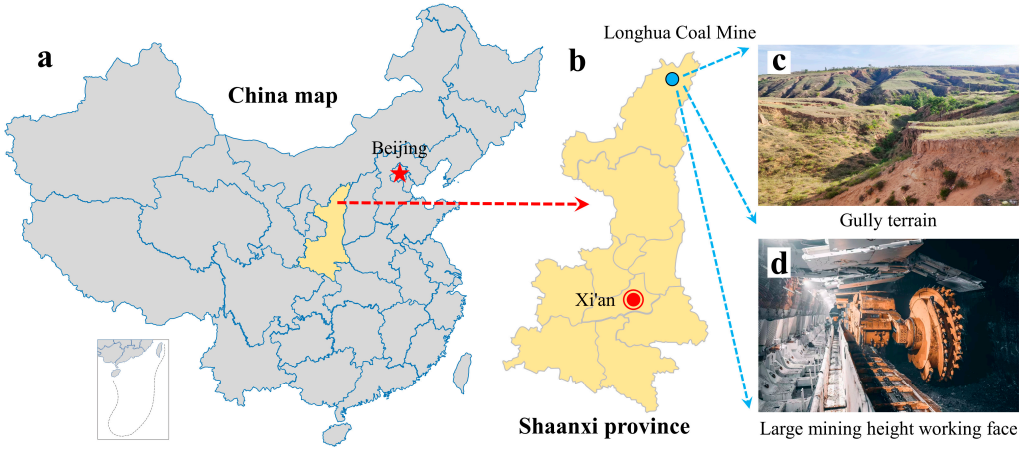


**Figure 1.** Overview of the study area: (**a**) geographic location of the northern Shaanxi mining area; (**b**) location of the Longhua Mine; (**c**) gully terrain on the surface; (**d**) 20202 large mining height working face.

The 20202 working face adopts a headentry, tailentry, and subsidiary transportation roadway arrangement, and all three roadways are arranged along the floor of the $2^{-2}$ coal seam. Among them, the tailentry is arranged on one side of the face, the headentry and subsidiary transportation roadway are arranged in parallel on the other side of the face, and a 15 m wide coal pillar is left between the two roadways. After the 20202 working face is mined back, the subsidiary transport roadway is kept as the tailentry of the 20203 working face. Therefore, the total service period of the coal pillar includes the first mining period of the 20202 face and the second mining period of the 20203 working face. The roadway layout of the 20202 working face is shown in Figure 2.

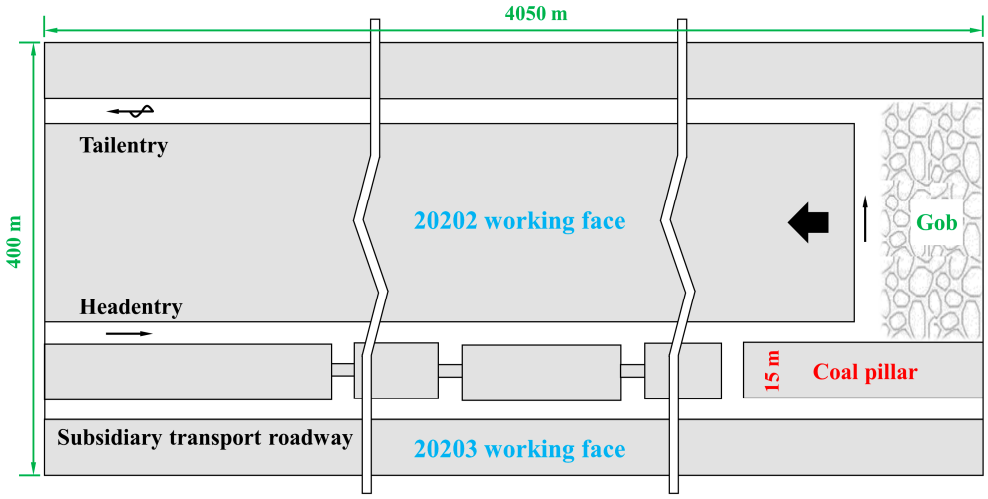


**Figure 2.** 20202 working face roadway layout.

The $2^{-2}$ coal seam is a stable coal seam. The roof is mostly siltstone and medium grained sandstone, with undeveloped fractures, and belongs to the roof of class II to III, which is medium and difficult to fall. The floor is mostly siltstone and mudstone, and the results of the key stratum judgment show that the overlying strata of the 20202 working

face is a multi-key strata structure containing a composite key stratum [24]. The borehole histogram of the 20202 working face is shown in Figure 3.

| Borehole column | Lithology | Thickness (m) |
|---|---|---|
| | Loess formation | 22~86 |
| | Fine grained sandstone | 40.8 |
| | Siltstone | 9.5 |
| | Fine-siltstone interbedding | 16.2 |
| | Medium grained sandstone | 4.2 |
| | Siltstone | 9.7 |
| | Compound main roof | 17.9 |
| | Siltstone | 4.2 |
| | $2^{-2}$ coal seam | 6.5 |
| | Siltstone | 19 |

**Figure 3.** Borehole histogram of 20202 working face.

### *2.2. UAV Observation of the Topography of the Study Area*

In order to further clarify the topographic characteristics of the surface of the 20202 working face, according to the information of the Longhua Coal Mine Geological Assurance System, the study area was accurately located through satellite maps, and the DJI Phantom 4 Pro V2.0 UAV was used to observe the surface gully area of the working face, as shown in Figure 4.

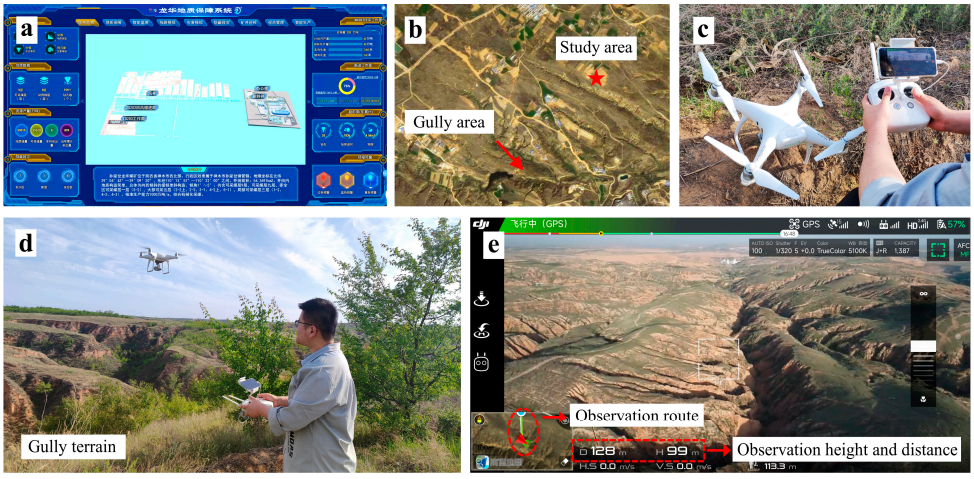


**Figure 4.** UAV observation of the topography of the study area: (**a**) Mine Geological Assurance System; (**b**) location demarcation of the study area (satellite map); (**c**) UAV assembly and navigation system debugging; (**d**) UAV observation; (**e**) remote control screen and parameter display.

Figure 5 shows the topographic characteristics of the study area. According to the UAV observation results, it can be seen that the surface of the 202 panel area is the gully area of the Loess Plateau, and the surface of the panel area can be obviously divided into the gully terrain area and the gentle terrain area, with the overall performance of the east and the north being gentle, the surface of the west and the south undulating more, and the surface of the southeast area being gullies and ravines, which is typical of the gully terrain. The panel area as a whole shows the characteristics of high in the west and low in the east, and high in the south and low in the north, with the surface height difference of about 64 m. Although the topography is gentle, the terrain is higher because of thick loess formation.

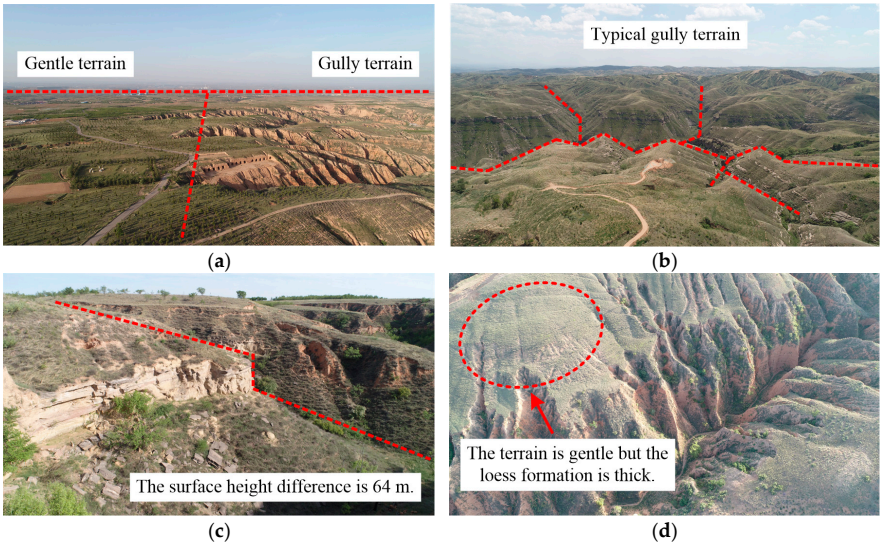


**Figure 5.** Observations of the topography of the study area: (**a**) gully terrain area and gentle terrain area; (**b**) typical gully terrain; (**c**) surface height difference observation; (**d**) gentle terrain area with thick loess formation.

### *2.3. Coal Pillar Stabilization Conditions and Design Principles*

The coal pillar size, anchoring method, and stress level all have great influence on the damage degree of the coal pillar [9,25,26], and it is difficult to accurately judge the damage condition of the coal pillar, so the damage degree of the coal pillar can be defined via a quantitative description method under the condition of controlling variables. Taking the 20202 working face of Longhua Coal Mine as an example, keeping the coal pillar size, anchoring method, and bedrock conditions unchanged, the relationship between the size of the load borne by the coal pillar and the damage degree of the coal pillar under the conditions of different base load ratios (the ratio of the thicknesses of bedrock and loess formation) was analyzed by changing the thickness of the loess formation to determine the state of the coal pillar, as shown in Figure 6.

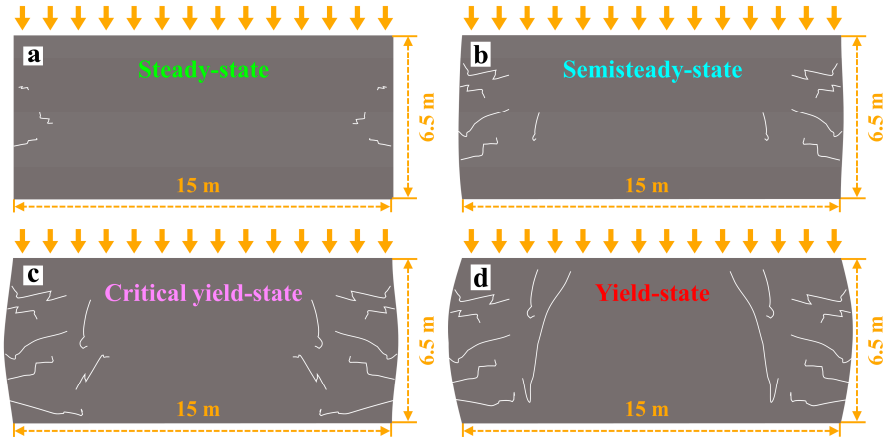


**Figure 6.** Schematic representation of coal pillar states at different damage levels: (**a**) steady state; (**b**) semi-steady state; (**c**) critical yield state; (**d**) yield state.

After the coal pillar is stressed, plastic and elastic zones will be generated, in which case the width of the elastic zone reflects the bearing capacity of the coal pillar, while the range of the plastic zone and the damage degree of the coal pillar can determine the state of the coal pillar [27]. As can be seen in Figure 6, with the gradual increase in the load transmitted by the overlying strata to the coal pillar, the coal pillar is gradually transformed from the steady state to the semi-steady state. The longitudinal fractures within the plastic

zone on both sides of the coal pillar can be considered to be in the critical yield state before penetration, reaching the critical point where the coal pillar remains stable. As the load continues to increase, the coal pillar enters the yield state; both sides of the coal pillar are completely destroyed, but the coal pillar still has a certain bearing capacity because of the incomplete elastic core zone [9,28].

Therefore, when the plastic zone at both sides of the coal pillar has local penetration, the coal pillar is relatively stable. When the plastic zone at both sides of the coal pillar is completely through and the overall force occurs, it means that the coal pillar terminates yielding [27]; although the force of the coal pillar at this time is uniform because of the secondary bearing, the deformation of the coal pillar and the roadway is larger, which is not suitable for the reasonable width of the coal pillar to be set up [19]. To summarize, the semi-steady state coal pillar close to the critical yield state is a more ideal width for coal pillar setting.

Combined with the geological conditions and the actual situation of the surface valley topography of Longhua Coal Mine, the following principles are proposed for determining the reasonable design width of the coal pillars in the 20202 working face:

(1) Consider the effect of the repeated mining at the working face on the damage degree to the coal pillar. Ensure that the coal pillar can be in a semi-steady state during the first mining period, and the coal pillar can still be in critical yield state during the second mining period.
(2) Consider the influence of the overlying strata base load ratio on the damage degree of the coal pillar. Determine the width of the coal pillar according to the actual overlying strata base load ratio of the working face to ensure that the coal pillar can still be in a critical yield state during the second mining period.
(3) Consider the influence of gully topography on the damage degree of the coal pillar. The thickness of the loess formation on the surface of the working face at different locations is different because of the topography of the gully. For the case of different base load ratio of the overlying strata caused by the topography of the gully, the actual maximum loess formation thickness should be used to convert the load under the fixed thickness of bedrock to ensure that the coal pillar can still be in the critical yield state during the second mining period.
(4) Consider the influence of the relative spatial position of the coal pillar and the gully slope sections on the damage degree of the coal pillar. If the coal pillar is below the gully topography, due to the fixed sequence of the first and the second mining periods of the coal pillar, it is necessary to discuss the damage degree and stability of the coal pillar when it is directly below different gully slope sections. On the one hand, the analysis results can be used as a reference basis for the determination of the coal pillar setting position and working face length in other working faces in the panel area, and on the other hand, they can be used to ensure that the relative position of the coal pillar below the gully slope section can still be in the critical yield state during the second mining period.

## 3. Fractal Characteristics of Coal Pillars with Different Overlying Strata Base Load Ratios in the Gentle Terrain Area

### *3.1. Numerical Model and Model Parameters*

According to the observation results of the topography, it can be seen that although part of the surface area of the 20202 working face of Longhua Coal Mine is gentle, the thickness of the loess formation is different in different areas, which makes the overlying strata base load ratio of the working face different in different areas. In order to study the damage characteristics of coal pillars with different overlying strata base load ratios in gentle terrain, a PFC$^{2D}$ numerical model was established.

The PFC$^{2D}$ particle flow code discrete element software can visualize the development process and distribution characteristics of fractures in the coal pillar after first and second mining, which is an effective tool to study the damage degree of coal pillars. A PFC$^{2D}$

numerical model with a length of 145 m and a height of 128 m was established according to the conditions of the coal seams and rock strata at the 20202 working face, in which the thickness of bedrock above the coal seam was 102.5 m, and the thickness of the loess formation was converted to the load applied above the model. The model was designed with six sets of operation schemes with different overlying strata base load ratios, and different thicknesses of the loess formation were simulated by changing the loads applied above the model.

Using the JL-REPT(A) rock elastic mechanical parameter in situ testing system of the State Key Laboratory of Coal Mine Disaster Dynamics and Control of Chongqing University to conduct in situ testing in the underground field, and combined with the research information of the neighboring mines and the papers under similar conditions, the mechanical parameters of the coal and rock in each rock strata of the 20202 working face were comprehensively obtained [29,30]. The mesoscopic interface parameters of the model are shown in Table 1, and parallel bonding between particles was used. DFN was used to record the actual fractures between the particles during the model operation process, which were naturally piled up under the gravity field until full equilibrium.

**Table 1.** Mesoscopic interface parameters for the particle flow code numerical model.

| Lithology | Elastic Modulus (Gpa) | Shear Modulus (Gpa) | Friction Angle (°) | Cohesion (Mpa) | Tensile Strength (Mpa) |
|---|---|---|---|---|---|
| loess formation | 0.15 | 0.13 | 9.00 | 0.26 | 0.04 |
| fine grained sandstone | 8.56 | 7.42 | 38.89 | 3.08 | 1.09 |
| siltstone | 4.86 | 4.17 | 42.03 | 4.23 | 1.87 |
| fine-siltstone interbedding | 13.54 | 12.03 | 41.22 | 4.85 | 3.31 |
| medium grained sandstone | 18.77 | 15.12 | 43.54 | 5.21 | 4.13 |
| siltstone | 8.44 | 6.93 | 42.08 | 4.31 | 2.12 |
| compound main roof | 12.04 | 10.23 | 33.47 | 4.29 | 3.13 |
| siltstone | 7.92 | 6.42 | 41.87 | 4.28 | 2.07 |
| $2^{-2}$ coal seam | 4.57 | 3.43 | 35.46 | 4.91 | 0.42 |
| siltstone | 9.94 | 8.13 | 42.07 | 4.59 | 2.08 |

After the model was established, a headentry and subsidiary transportation roadway with a height of 4.5 m and a width of 6.2 m were set up in the middle area of the model along the bottom of the coal seam, a coal pillar with a height of 6.5 m and a width of 15 m was set up between the two roadways, and 24 measuring points were arranged uniformly in the coal pillar to monitor the change in the porosity of the coal pillar. The modeling results of the right-hand side of the coal pillar after the mining of the 20202 working face were operated first, and then the results of the left-hand side of the model after the mining of the 20203 working face were operated. The establishment of the numerical model and the mining scheme are shown in Figure 7.

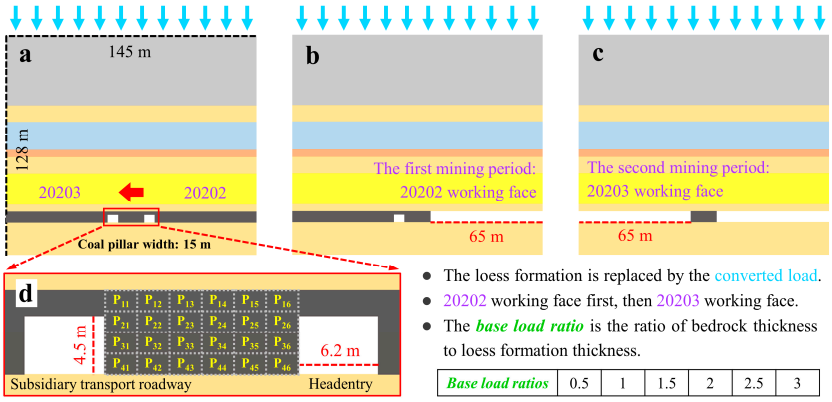


**Figure 7.** PFC$^{2D}$ numerical model and measurement points layout: (**a**) roadway excavation period; (**b**) first mining period; (**c**) second mining period; (**d**) measurement points layout scheme.

### 3.2. Fractal Characteristics of Coal Pillar Fractures

Fractal theory can accurately characterize the irregularity degree of fractures, and is an effective method to describe the nonlinear development characteristics of fractures and the damage degree of coal pillars [19,30]. In this study, the fractal dimension was calculated using the counting box dimension method, and the calculation principle aims to cover the fracture network within the coal pillar with a certain side length of the square grid, calculate the number of square grids required to cover all the fracture network, enlarge or reduce the size of the square grid proportionally, and calculate the number of square grids required to cover the fracture network in turn, so that a set of one-to-one correspondence between the side lengths of the square grids $r$ and the number $N$ is obtained [21,22,31], and then can be calculated by Equation (1).

$$D_f = \lim \frac{\lg N(r)}{-\lg r} \tag{1}$$

Six numerical modeling schemes with different overlying strata base load ratios were operated separately, the fracture images of the coal pillars were binarized, and the fractal dimension was used to characterize the development and complexity of the fractures in the coal pillars and to establish the quantitative relationship between the overlying strata base load ratio and the fractal dimension. Considering that the number of fractures within the coal pillar in the numerical simulation results may be small, which brings difficulties to the calculation of the fractal dimension, it is also easy for this method to lead to error in the calculation results. Therefore, in this paper, the faclab plug-in of the Matlab program is utilized to count the number of boxes $N$ at different radii, $D_f$ [29,32]. The distribution characteristics of the fractures and the fractal dimension results within the coal pillar under different overlying strata base load ratios are shown in Figure 8.

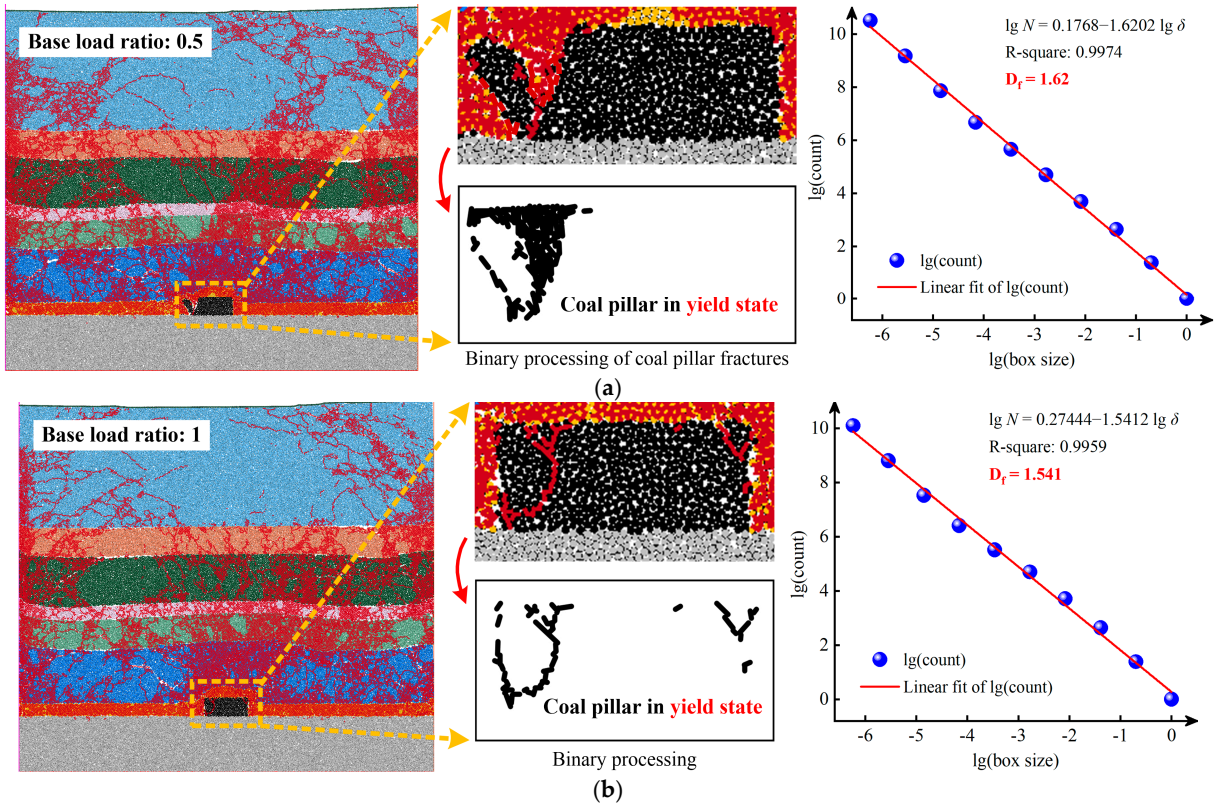


**Figure 8.** *Cont.*

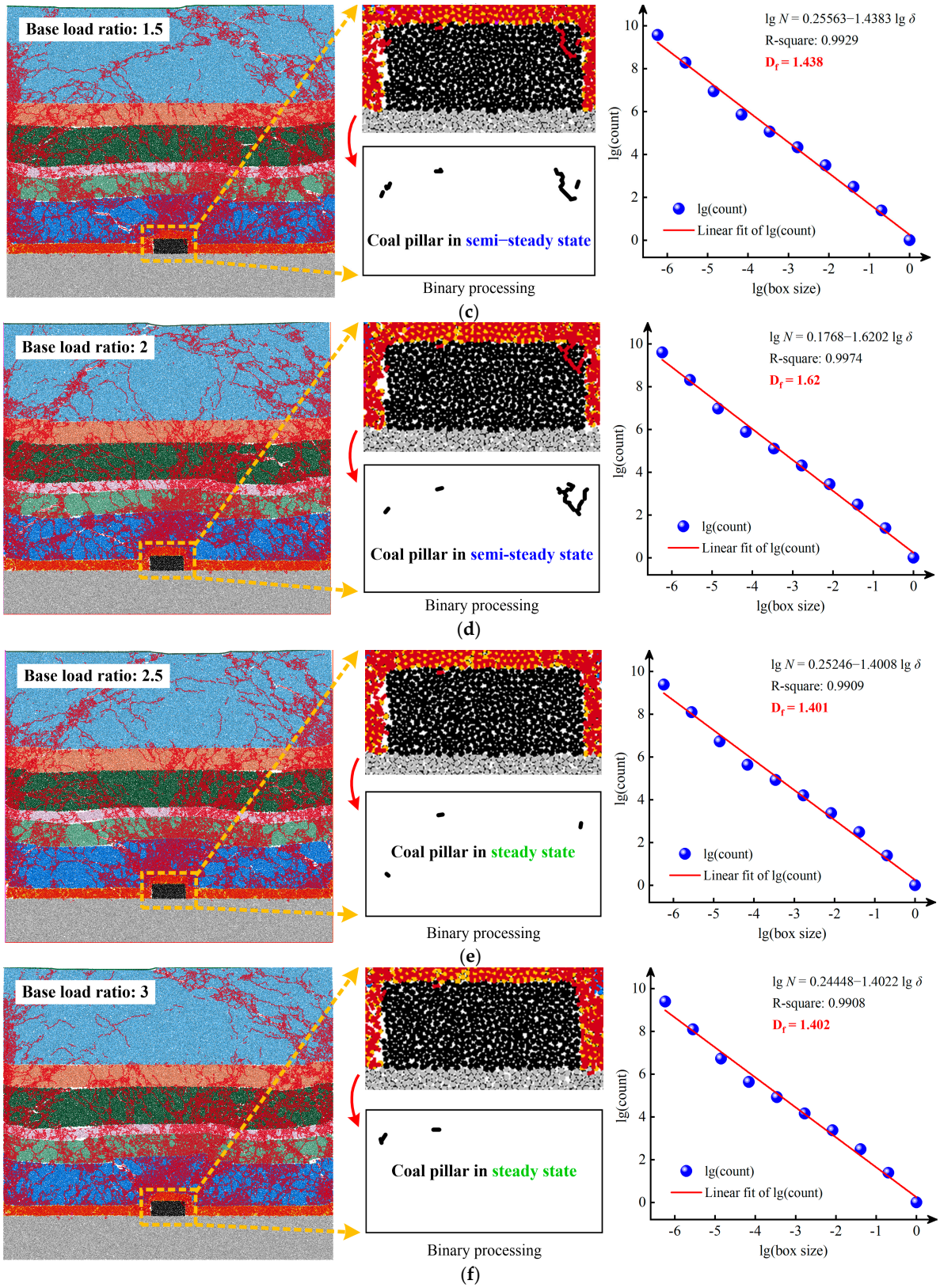


**Figure 8.** Distribution characteristics and fractal dimensions of fractures in coal pillars under different overlying strata base load ratios: (**a**) base load ratio: 0.5; (**b**) base load ratio: 1; (**c**) base load ratio: 1.5; (**d**) base load ratio: 2; (**e**) base load ratio: 2.5; (**f**) base load ratio: 3.

As can be seen in Figure 8, with the increase in the overlying strata base load ratio, the fractal dimension and damage degree of the coal pillar gradually become smaller, and the

coal pillar is more stable. According to the stable condition of the coal pillar, the state of the coal pillar under different overlying strata base load ratios was determined when the overlying strata base load ratio was less than 1, the coal pillar was in the yield state, and the coal pillar near the 20203 working face had a large damage degree, and the whole coal pillar was unstable at this time, which means that the width of the coal pillar should be increased or reinforcement measures should be taken when the loess formation thickness is more than 102.5 m. The coal pillar will be more stable when the overlying strata base load ratio increases, or reinforcement measures should be taken for the coal pillar. When the overlying strata base load ratio is more than 2.5, the coal pillar is in a steady state, and the integrity of the coal pillar is better because the fractures are not developed; then, the width of the coal pillar can be further reduced, so as to reduce the waste of coal resources [12]. From the results of the fractal dimension of the fractures within the coal pillar, it can be seen that when the fractal dimension is less than 1.38 and more than 1.54, the width of 15 m for the coal pillar is unreasonable.

### *3.3. The Number of Fractures and Characteristics of Porosity Evolution within the Coal Pillar*

In order to analyze the development of fractures within the coal pillar under different base load ratios, the number of fractures within the coal pillar in the numerical simulation results was derived and compared to obtain the interval of the number of fractures corresponding to the different coal pillar states. The number of fractures within the coal pillar of the six sets of simulation schemes is shown in Figure 9.

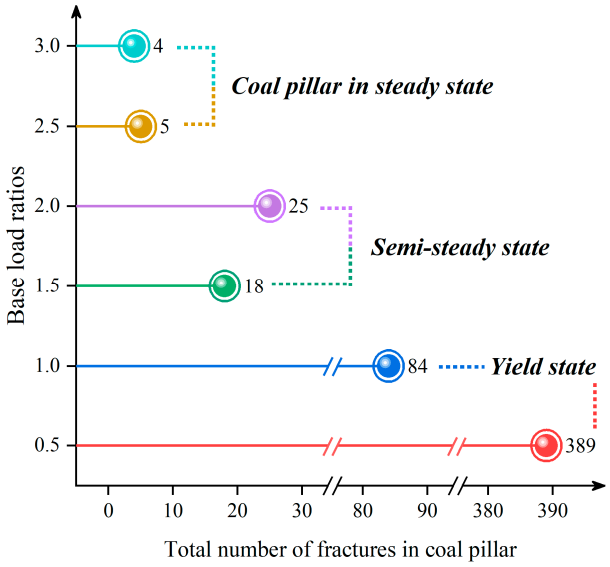


**Figure 9.** Number of fractures within coal pillars under different overlying strata base load ratios.

Figure 9 demonstrates the correspondence between the number of fractures within the coal pillar and the state of the coal pillar under six overlying strata base load ratio conditions. In general, the coal pillar is in the steady state when the number of fractures within the coal pillar is less than 10, the coal pillar is in the semi-steady state when the number of fractures within the coal pillar is 10–25, the coal pillar is in the critical yield state when the number of fractures within the coal pillar is 26–35, and the coal pillar is in the yield state when the number of fractures within the coal pillar is more than 35.

In order to further analyze the relationship between the overlying strata base load ratio and the damage degree of the coal pillar, the coal pillar porosity monitoring data of the measuring points after the end of numerical modeling operation were exported, and the contour cloud map of the coal pillar porosity was plotted and labeled with the porosity data of each measuring point, as shown in Figure 10.

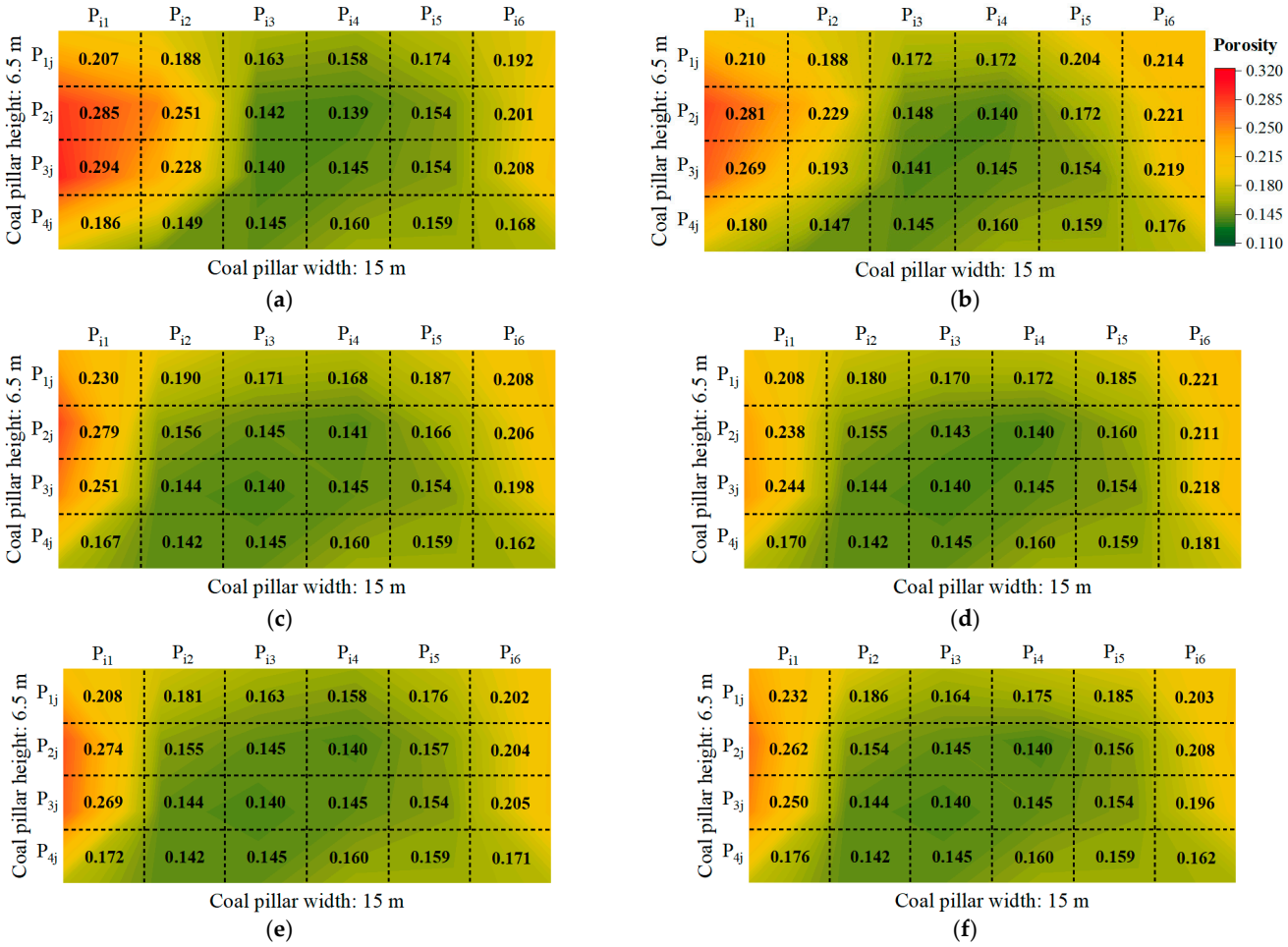


**Figure 10.** Porosity distribution within the coal pillars at different overlying strata base load ratios: (**a**) base load ratio: 0.5; (**b**) base load ratio: 1; (**c**) base load ratio: 1.5; (**d**) base load ratio: 2; (**e**) base load ratio: 2.5; (**f**) base load ratio: 3.

As can be seen in Figure 10, with the increase in the overlying strata base load ratio, the increase in the porosity within the coal pillar is smaller. Among all the simulation results, the porosity increase is more obvious in the monitoring areas of $p_{11}$, $p_{21}$, $p_{31}$, $p_{16}$, and the porosity in the area close to the 20203 working face is larger, which indicates that the left-hand side of the coal pillar is more damaged. When the overlying strata base load ratio is 0.5 and 1, the coal pillar is in the yield state, and besides the four measuring points, the porosity increase in the two measuring points, $p_{22}$, $p_{32}$, is also larger.

### *3.4. Discussion*

Through the analysis of the fractal characteristics, fracture number, and porosity evolution characteristics of the coal pillar, it can be found that the overlying strata base load ratio has a great influence on the development and distribution of the internal fracture of the coal pillar, which directly determines the damage degree and stability of the coal pillar. Overall, the damage degree of the coal pillar is always greater near the side of the 20203 working face, and after analyzing the reason, the mining disturbance of the 20202 working face has made the coal pillar near the side of the 20203 working face appear to have an obvious stress concentration, so at this time, the coal pillar area on the side of the 20203 working face is in the state of continuous bearing, which is easier to be destroyed after the 20203 working face is mined back [25].

In order to visualize and analyze the influence of the overlying strata base load ratio on the development of coal pillar fractures, the results of fractures in the coal pillars under

different overlying strata base load ratio conditions were counted, as shown in Table 2. The fractal dimension of the fractures in the coal pillar under different overlying strata baseload ratios was fitted, and the relationship equation between the overlying strata base load ratio and the fractal dimension was obtained, as shown in Figure 11.

**Table 2.** Fracture results within the coal pillars at different overlying strata base load ratios.

| Base Load Ratio | Loess Formation Thickness (m) | Fractal Dimension $D_f$ | Correlation Coefficient | Fracture Number | Coal Pillar State |
|---|---|---|---|---|---|
| 0.5 | 205 | 1.620 | 0.9974 | 389 | yield state |
| 1 | 102.5 | 1.541 | 0.9959 | 84 | yield state |
| 1.5 | 68.33 | 1.438 | 0.9929 | 18 | semi-steady state |
| 2 | 51.25 | 1.448 | 0.9936 | 25 | semi-steady state |
| 2.5 | 41 | 1.401 | 0.9909 | 5 | steady state |
| 3 | 34.17 | 1.402 | 0.9908 | 4 | steady state |

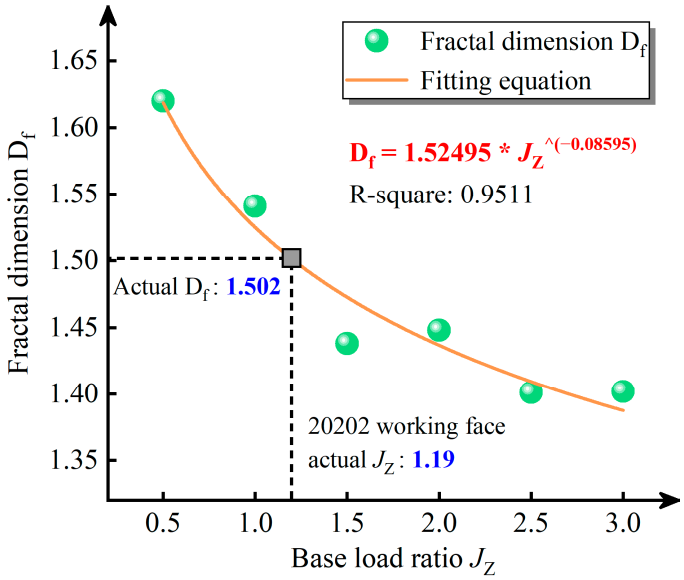


**Figure 11.** Fitting equation for overlying strata base load ratios to fractal dimensions of fractures within coal pillars.

As can be seen from Table 2 and Figure 11, the smaller the overlying strata base load ratio is, the more the number of fractures in the coal pillar is, and the larger the fractal dimension is. There is a mathematical relationship between the overlying strata base load ratios and the fractal dimensions of the fractures within coal pillars, and the fitting equation can be obtained as follows:

$$D_f = 1.52495 \times J_Z^{\wedge(-0.08595)}. \quad (2)$$

Through this fitting equation, the fractal dimension of the fractures within the coal pillar at the actual minimum overlying strata base load ratio (1.19) in the 20202 working face of Longhua Coal Mine could be calculated to be 1.502. In order to verify the reliability of the fitting equation, the bedrock parameters of the numerical model were kept unchanged, the 86 m loess formation was converted to the corresponding load value and applied to the numerical model, the results of the numerical simulation were exported, the image of the fractures within the coal pillar was binarized, and the fractal dimension was calculated to analyze the distribution characteristics of the porosity within the coal pillar, as shown in Figure 12.

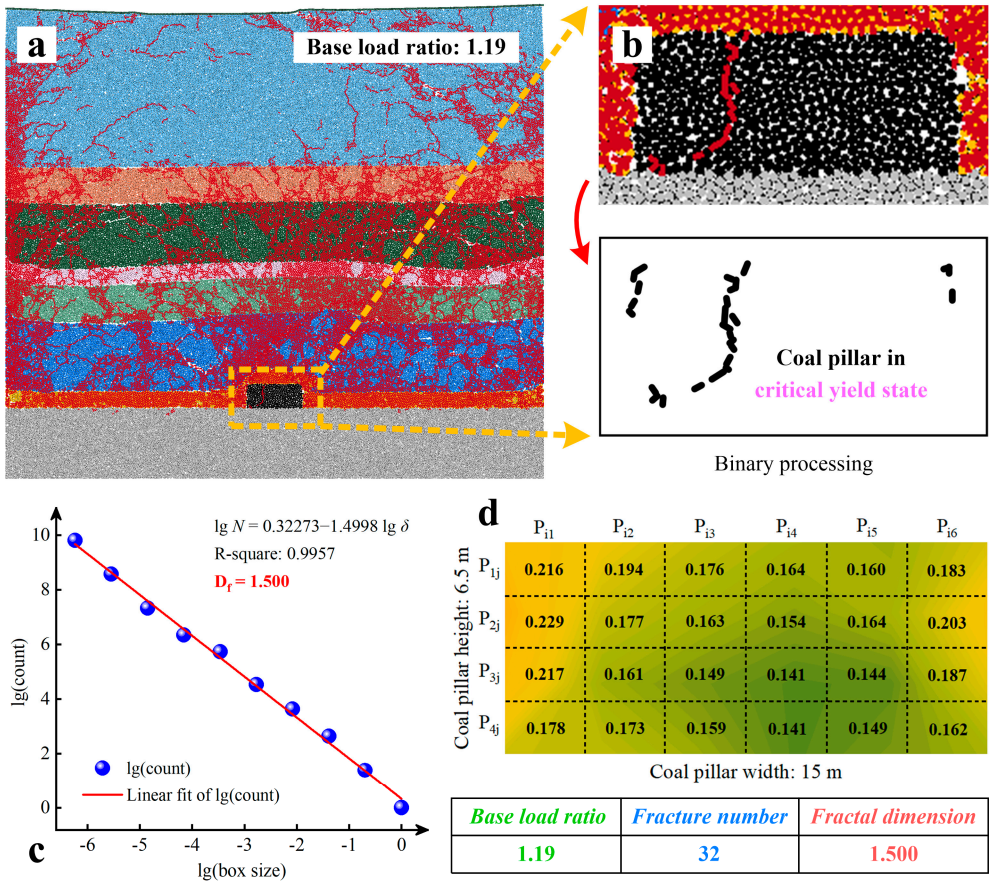


**Figure 12.** Numerical simulation results and the distribution characteristics of the fractures within the coal pillar for an overlying strata base load ratio of 1.19: (**a**) numerical simulation results; (**b**) distribution of fractures within the coal pillar and binarization; (**c**) fractal dimension of the fractures within the coal pillar; (**d**) porosity distribution within the coal pillar.

As can be seen from Figure 12, when the overlying strata base load ratio is 1.19, the fractal dimension of the fractures within the coal pillar obtained by numerical simulation is 1.500, which is basically the same as that of 1.502 calculated via the fitting equation, which shows that the accuracy and reliability of the fitting equation are high. At the same time, according to the modeling results, the number of fractures and porosity distribution within the coal pillar is also between the overlying strata base load ratio of 1.0 and 1.5, at which time the coal pillar is in the critical yield state.

Overall, calculating the fractal dimensions of the fractures in the coal pillars has a positive significance in determining the damage degree of the coal pillars under the conditions of different overlying strata base load ratios, and the fitting equation of the overlying strata base load ratios and the fractal dimensions of the fractures in the coal pillar can also be effective in determining the damage degree of the coal pillar corresponding to the unknown loess formation thickness.

## 4. Damage Law of Coal Pillars under Different Gully Slope Sections in the Gully Terrain Area

### *4.1. Numerical Model*

According to the results of the topographic observation, the surface of the Longhua Coal Mine 20202 working face is a typical gully terrain, and the height difference of the surface is about 64 m. The damage degree of coal pillars under different gully slope sections is different. In order to study the damage characteristics of coal pillars under different gully slope sections in gully terrain area, a PFC$^{2D}$ numerical model was established. The bedrock conditions, parameter settings, measuring points arrangement, and mining scheme of the

model are consistent with the numerical model shown in Figure 7, and only the setting scheme of the loess formation was changed. Considering the fixed nature of the mining sequence of the 20202 and 20203 working faces, a total of four sets of model operation schemes were designed according to the actual situation to simulate the bearing condition and damage degree of the coal pillars located underneath the peak of the gully, gully bottom, upslope section of the gully, and downslope section of the gully, respectively, where the thickness of the gully bottom of the loess formation was about 22 m, and the thickness of the peak of gully was about 86 m. The numerical modeling scheme is shown in Figure 13.

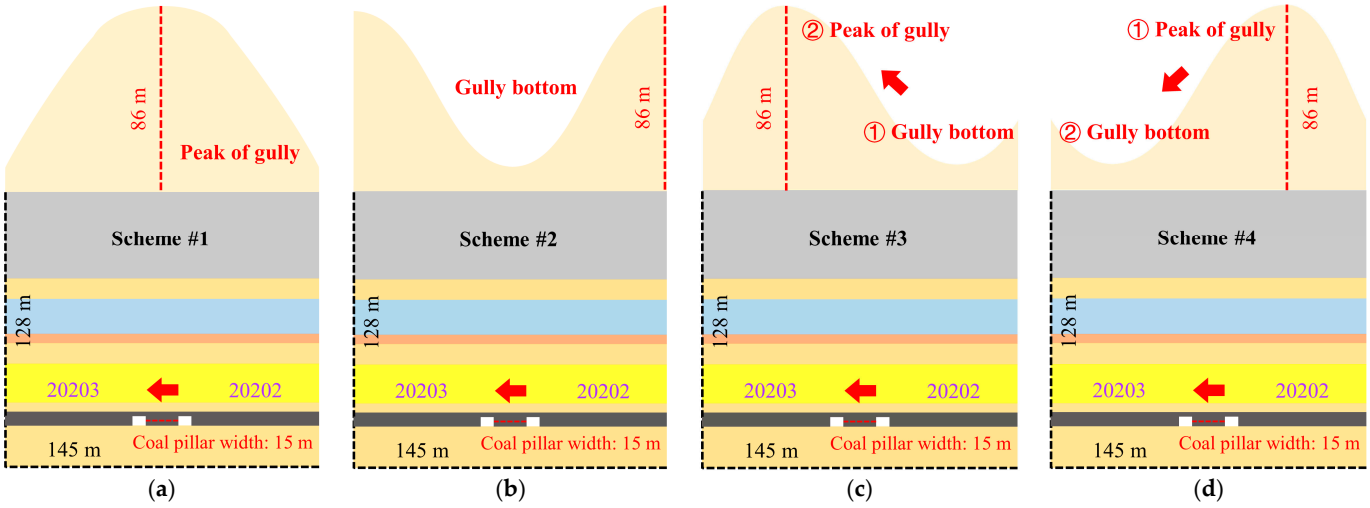


**Figure 13.** PFC$^{2D}$ numerical modeling schemes: (**a**) coal pillar below the peak of the gully; (**b**) coal pillar below the gully bottom; (**c**) coal pillar below the upslope section of the gully; (**d**) coal pillar below the downslope section of the gully.

### *4.2. Fractal Characteristics of Coal Pillar Fractures*

Numerical modeling schemes for four sets of coal pillars located under different gully slope sections were operated separately, and the fracture images of the coal pillars were binarized to calculate the fractal dimensions of the fractures within the pillars, as shown in Figure 14.

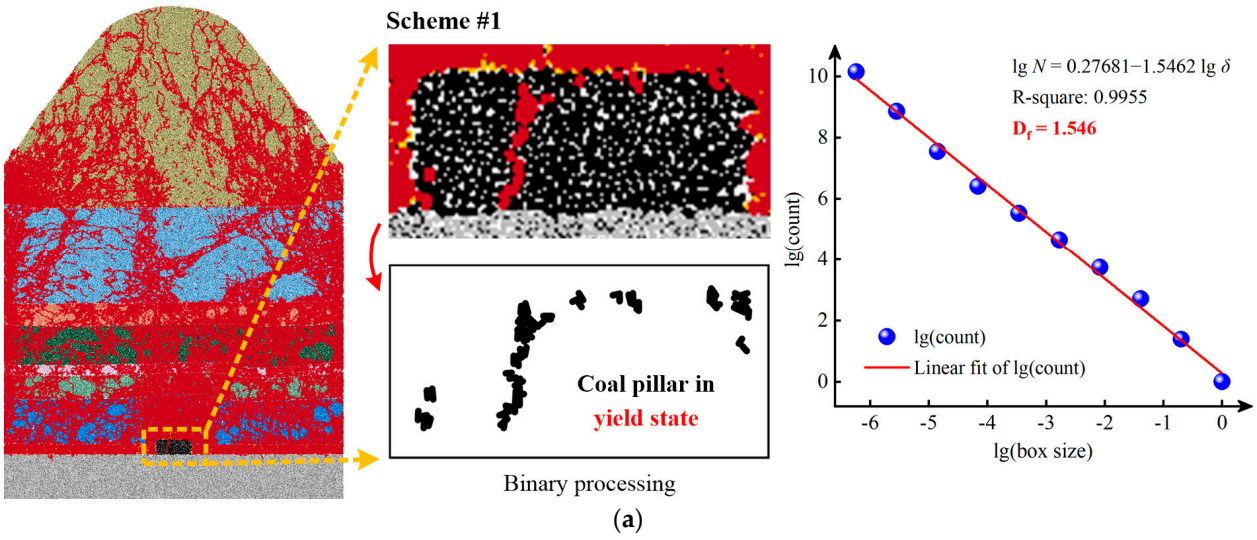


**Figure 14.** *Cont.*

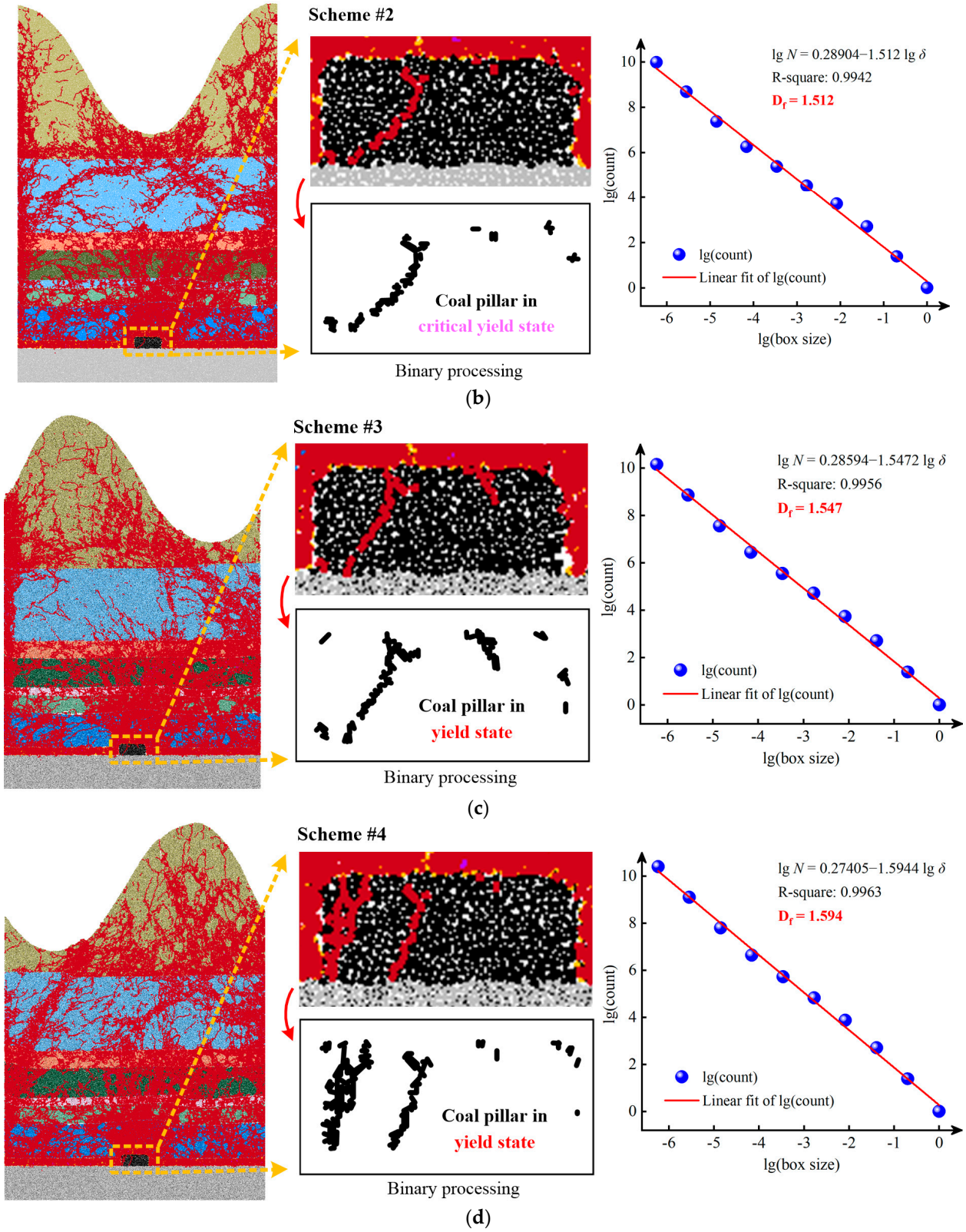


**Figure 14.** Distribution characteristics and fractal dimensions of fractures within the coal pillars when located below different gully slope sections: (**a**) coal pillar below the peak of the gully; (**b**) coal pillar below the gully bottom; (**c**) coal pillar below the upslope section of the gully; (**d**) coal pillar below the downslope section of the gully.

As can be seen in Figure 14, only when the coal pillar is located below the gully bottom (scheme #2), is the coal pillar in the critical yield state, and the coal pillars in the rest of the schemes are in the yield state; it can be seen that the damage degree of the coal pillar in the gully terrain area is obviously larger than that in the gentle terrain area. According to the results of fractal dimension calculation, the damage degree of the coal pillar is the largest when it is located below the downslope section of the gully ($D_f$ = 1.594), followed by the coal pillar located below the peak of the gully ($D_f$ = 1.546) and the upslope section of the gully ($D_f$ = 1.547), and the damage degree of the coal pillar is the smallest when it is located below the bottom of the gully ($D_f$ = 1.512).

Meanwhile, according to the stabilization conditions of the coal pillar, it can be seen that when the coal pillar is located below the gully bottom in the gully terrain area, the width of the coal pillar of 15 m is more reasonable, while the other schemes need to increase the width of the coal pillar or take reinforcing measures for the coal pillar.

### *4.3. The Number of Fractures and Characteristics of Porosity Evolution within the Coal Pillar*

In order to analyze the development of fractures within the coal pillar when it is located below different gully slope sections, the number of fractures within the coal pillar in the numerical simulation results is derived, as shown in Figure 15.

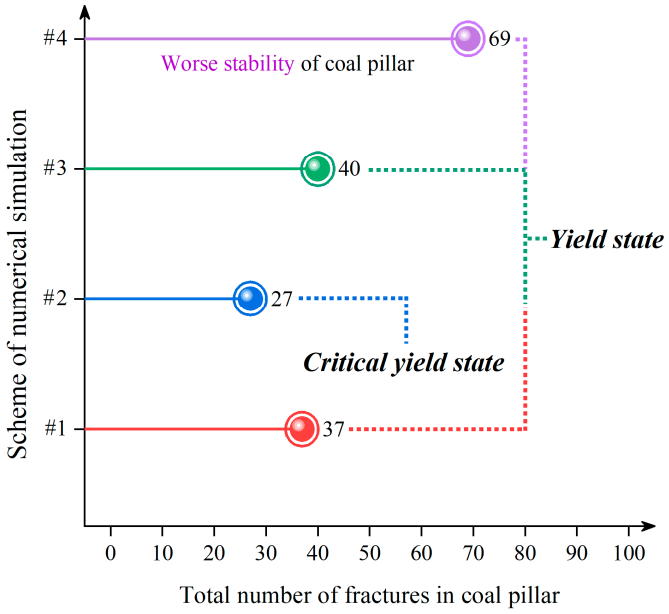


**Figure 15.** Number of fractures and corresponding states within coal pillars when located below different gully slope sections.

Figure 15 shows the correspondence between the number of fractures within the coal pillar and the state of the coal pillar when it is located below different gully slope sections. The number of fractures within the coal pillar is 27 when the coal pillar is located below the gully bottom and the coal pillar is in the critical yield state, while the number of fractures within the coal pillar in the remaining three schemes is greater than 35 and the coal pillar is in the yield state, which is in line with the interval of the number of fractures corresponding to the different coal pillar states obtained above.

In order to further analyze the damage degree of the coal pillar when it is located below different gully slope sections, the coal pillar porosity monitoring data of the measuring points after the end of numerical modeling operations are derived, and the contour cloud map of the coal pillar porosity is plotted and labeled with the porosity data of each measuring point, as shown in Figure 16.

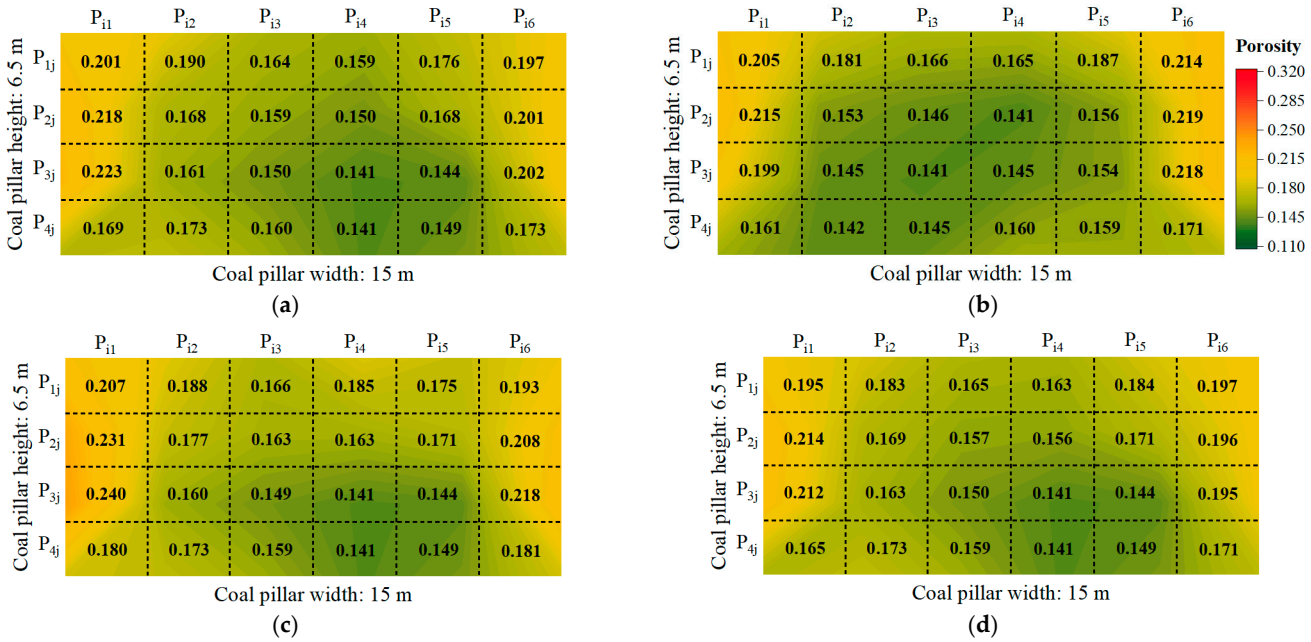


**Figure 16.** Porosity distribution within the coal pillar at different gully slope sections: (**a**) coal pillar below the peak of the gully; (**b**) coal pillar below the gully bottom; (**c**) coal pillar below the upslope section of the gully; (**d**) coal pillar below the downslope section of the gully.

As can be seen in Figure 16, the porosity within the coal pillar below the gully bottom is small, and the porosity growth rate and growth area within the coal pillar obtained from the other three simulation schemes are basically the same. Generally speaking, the porosity in the six monitoring areas of $p_{11}$, $p_{21}$, $p_{31}$, $p_{16}$, $p_{26}$, $p_{36}$ is larger, and the porosity in the area near the 20203 working face is larger than that near the 20202 working face, but the difference in porosity between the two sides of the coal pillar is relatively small. This indicates that both sides of the coal pillar have different degrees of damage.

### *4.4. Discussion*

In order to visually analyze the fracture development of the coal pillar when it is located below different gully slope sections, the fracture results within the coal pillar obtained from the four numerical simulation schemes were counted, as shown in Table 3.

**Table 3.** Fracture results within coal pillars when located below different gully slope sections.

| Scheme Order | Gully Slope Section | Fractal Dimension $D_f$ | Correlation Coefficient | Fracture Number | Coal Pillar State |
|---|---|---|---|---|---|
| #1 | peak of the gully | 1.546 | 0.9955 | 37 | yield state |
| #2 | gully bottom | 1.512 | 0.9942 | 27 | critical yield state |
| #3 | upslope section of the gully | 1.547 | 0.9956 | 40 | yield state |
| #4 | downslope section of the gully | 1.594 | 0.9963 | 69 | yield state |

Through the analysis of the fractal characteristics, fracture number, and porosity evolution of the coal pillars, it can be found that the damage degree of the coal pillars is different when they are located below different gully slope sections. Among the four sets of simulation results, the damage degree of the coal pillar located below the downslope section of the gully is the largest, and the damage degree of the coal pillar located below the gully bottom is the smallest. At this time, the thickness of the loess formation above the coal pillar is only 22 m, but the number of fractures and fractal dimension within the coal pillar are similar to the simulation results obtained when the thickness of the loess formation is 86 m (base load ratio: 1.19). This indicates that the damage degree of the coal

pillars is greater in the gully terrain area. After analyzing the reason, it is mainly because in the first mining period, in addition to the load transferred from the overlying strata to the coal pillar, the loess formation of the peak of the gully slipped to the downslope side of the gully after the mining of the 20202 working face, which resulted in the further increase in the load borne by the coal pillar, and thus it is easier to be destabilized in the second mining period [33–35]. In general, compared with the gentle terrain area, the damage degree of the coal pillar in the gully terrain area is greater, and the bearing law and the fracture development law of the coal pillar are more complicated.

## 5. Coal Pillar Design Strategy Based on the Fractal Characteristics of Fractures

In underground mining activities, the coal pillar is an important structure to control the stability of the surrounding rock of the roadway and to maintain the safety of the mining operations. A small width of coal pillar is easy to destabilize and become damaged, while a large width of coal pillar will cause a large amount of coal resources to be wasted. Therefore, on the basis of ensuring the safety of working face mining, determining the reasonable width of coal pillars is a technical problem that needs to be solved urgently in mines, which is also in line with the development needs of green mining and scientific mining [15,23].

The fractal dimension and the number of fractures within the coal pillar can intuitively reflect the stability of the coal pillar, which is an effective method to quantify the damage degree of the coal pillar. According to the coal pillar stability conditions and numerical simulation results, the process for determining a reasonable coal pillar width design strategy based on the fractal characteristics of the fractures is shown in Figure 17.

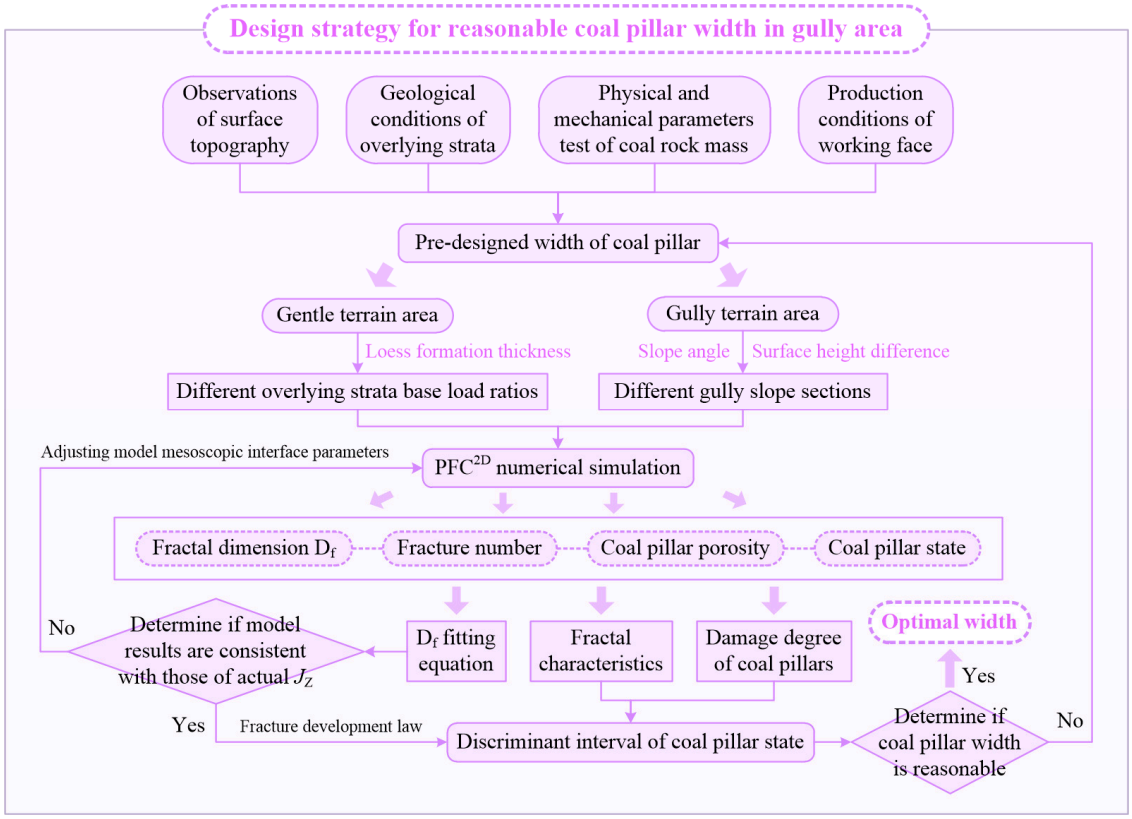


**Figure 17.** Process for determining reasonable coal pillar width design strategy.

As can be seen in Figure 17, in order to solve the problem of the coal pillar width design when mining shallow buried coal seams in the gully area, on the basis of clarifying the overlying strata geological conditions and surface topographic features, the mathematical relationship between the number of fractures and fractal dimensions of coal pillars and

the state of coal pillars under the conditions of different overlying strata base load ratios and gully slope sections were determined by numerical simulation, and the corresponding coal pillar width design strategy was proposed, which can provide a basis for determining the reasonable width of the coal pillars. Among them, the discriminant interval of coal pillar state is an important indicator for determining the damage degree of the coal pillar, and taking the 20202 working face of Longhua Coal Mine as an example, the discriminant intervals of coal pillar states were determined, as shown in Table 4.

**Table 4.** Discriminant intervals for the number of fractures and fractal dimensions under different coal pillar states.

| Type | Steady State | Semi-steady State | Critical Yield State | Yield State |
|---|---|---|---|---|
| fracture number | <10 | 10~25 | 26~35 | >35 |
| fractal dimension $D_f$ | <1.420 | 1.420~1.499 | 1.500~1.535 | >1.535 |

In summary, based on the coal pillar stability conditions and design principles, the fractal dimensions of the fractures in the coal pillars, combined with the distribution area and plastic zone range of the fractures in the coal pillars, the damage area and damage degree of the coal pillars can be effectively determined, which provides a positive strategy for the determination of the reasonable coal pillar width, and has also achieved good application effects in engineering practice, so the coal pillar design strategy can be adopted in other coal mines with similar geological conditions.

## 6. Conclusions

According to the geological conditions of the 20202 working face in Longhua Coal Mine, the stability conditions and design principles of the coal pillars in shallow buried coal seams in the gully area were analyzed and PFC$^{2D}$ numerical models were established, and the damage characteristics of coal pillars in different overlying strata base load ratios of gentle terrain area and different gully slope sections in gully terrain area were studied, respectively. A coal pillar width design strategy based on the fractal characteristics of the fractures was proposed, which can provide a reference for the determination of the coal pillar width under similar geological conditions. This study led to the following conclusions.

(1) Through UAV observation of the topography of the study area, the surface topographic features of the 20202 working face were determined. On this basis, the stability conditions and design principles of coal pillars were proposed, and the coal pillars were classified into four states, namely steady state, semi-steady state, critical yield state, and yield state, according to the damage degree of the coal pillars. The effects of repeated mining in the working face, the overlying strata base load ratio, the topography of the gully, and the relative spatial position of the gully slope section on the damage degree and stability of the coal pillars were considered to ensure that the coal pillars would be stable during the second mining period.

(2) The PFC$^{2D}$ numerical model was established under the conditions of different overlying strata base load ratios in the gentle terrain area, and the mathematical relationship between the overlying strata base load ratios and the fractal dimensions of the fractures in the coal pillars was obtained, and the corresponding fitting equation was established, which basically conformed to the results of the fractal dimension of the fractures in the coal pillar in the numerical simulation of the actual base load ratio of the 20202 working face, and proved the reliability of the fitting equation. The simulation results show that the damage degree of the coal pillar near the side of the 20203 working face is greater after the second mining period, and the coal pillar is basically in the critical yield state under the condition of the actual overlying strata base load ratio (1.19), which indicates that the width of 15 m for the coal pillar is more reasonable.

(3) The numerical simulation results for different gully slope sections in the gully terrain area show that the damage degree of the coal pillar in the gully terrain area is larger than that in the gentle terrain area, and the laws of coal pillar bearing and fracture development are more complicated. Among them, the fractal dimension of the fractures in the coal pillar located below the downslope section of the gully is the largest, and the fractal dimension of the fractures in the coal pillar located below the gully bottom is the smallest, so the coal pillar can be kept below the gully bottom as much as possible by changing the length of the working face, so as to ensure the stability of the coal pillar.

**Author Contributions:** Conceptualization, Z.W. and Y.L.; methodology, Q.R. and K.M.; software, Z.W. and Q.L.; formal analysis, W.S.; investigation, Z.W. and H.Y.; data curation, Y.L.; writing—original draft preparation, Z.W. and Y.M.; writing—review and editing, S.L. and K.M.; visualization, Z.W.; project administration, Y.M.; funding acquisition, Y.L. All authors have read and agreed to the published version of the manuscript.

**Funding:** This research was supported by the National Key R&D Program of China (Grant No. 2022YFC3004704), and the National Natural Science Foundation of China (52174166). These sources of support are gratefully acknowledged.

**Data Availability Statement:** The data generated and/or analyzed during this study are available from the corresponding author on reasonable request.

**Conflicts of Interest:** Dr. Hualong Yin and Dr. Yun Ma was employed by the Sunjiacha Longhua Mining Co., Ltd. The remaining authors declare that the research was conducted in the absence of any commercial or financial relationships that could be construed as a potential conflict of interest.

## References

1. Fang, G.; Liu, Y.; Liang, X.Y.; Huang, H. Hydrogeological characteristics and mechanism of a water-rich coal seam in the Jurassic coalfield, northern Shaanxi Province, China. *Arab. J. Geosci.* **2020**, *13*, 1088. [CrossRef]
2. Wei, J.B.; Wang, S.M.; Song, S.J.; Sun, Q.; Yang, T. Experiment and numerical simulation of overburden and surface damage law in shallow coal seam mining under the gully. *Bull. Eng. Geol. Environ.* **2022**, *81*, 207. [CrossRef]
3. Wang, M.; Xu, Y.L.; Xu, Q.Y.; Shan, C.F.; Li, Z.H.; Nan, H.; Li, Y.F.; Liu, H.L.; Chu, T.X. Stability control of overburden and coal pillars in the gob-side entry under dynamic pressure. *Int. J. Rock Mech. Min. Sci.* **2023**, *170*, 105490. [CrossRef]
4. Xu, X.H.; He, F.L.; Li, X.B.; He, W.R. Research on mechanism and control of asymmetric deformation of gob side coal roadway with fully mechanized caving mining. *Eng. Fail. Anal.* **2021**, *120*, 105097. [CrossRef]
5. Luo, P.; Zhang, Z.Y.; Zhang, L.; Liu, X.Q.; Liu, X.B. Influence of different $CO_2$ phase states on fluid flow pathways in coal: Insights from image reconstruction and fractal study. *Bull. Eng. Geol. Environ.* **2023**, *82*, 266. [CrossRef]
6. Zhang, Z.; Li, Z.; Xu, G.; Gao, X.J.; Liu, Q.J.; Li, Z.J.; Liu, J.C. Lateral abutment pressure distribution and evolution in wide pillars under the first mining effect. *Int. J. Min. Sci. Technol.* **2023**, *33*, 309–322. [CrossRef]
7. Yang, T.; Yang, Y.R.; Zhang, J.; Gao, S.S.; Li, T. Study on Development Law of Mining-Induced Slope Fracture in Gully Mining Area. *Adv. Civ. Eng.* **2021**, *3*, 1–9. [CrossRef]
8. Ran, Q.C.; Liang, Y.P.; Zou, Q.L.; Hong, Y.; Zhang, B.C.; Liu, H.; Kong, F.J. Experimental investigation on mechanical characteristics of red sandstone under graded cyclic loading and its inspirations for stability of overlying strata. *Geomech. Geophys. Geo-Energy Geo-Resour.* **2023**, *9*, 11. [CrossRef]
9. Li, Z.; Xu, J.L.; Ju, J.F.; Zhu, W.B.; Xu, J.M. The effects of the rotational speed of voussoir beam structures formed by key strata on the ground pressure of stopes. *Int. J. Rock Mech. Min. Sci.* **2018**, *108*, 67–79. [CrossRef]
10. Xu, J.L.; Zhu, W.B.; Wang, X.Z.; Zhang, Z.Q. Influencing mechanism of gully terrain on ground pressure behaviors in shallow seam longwall mining. *J. China Coal Soc.* **2012**, *37*, 179–185.
11. Liu, S.F.; Wan, Z.J.; Zhang, Y.; Lu, S.F.; Ta, X.P.; Wu, Z.P. Research on Evaluation and Control Technology of Coal Pillar Stability Based on the Fracture Digitization Method. *Measurement* **2020**, *158*, 107713. [CrossRef]
12. Wang, B.N.; Dang, F.N.; Gu, S.C.; Huang, R.B.; Miao, Y.P.; Chao, W. Method for determining the width of protective coal pillar in the pre-driven longwall recovery room considering main roof failure form. *Int. J. Rock Mech. Min. Sci.* **2020**, *130*, 104340. [CrossRef]
13. Song, C.H.; Lu, C.P.; Zhang, X.F.; Wang, C.; Xie, H.D.; Yan, X.Y.; Yang, H.W. Moment Tensor Inversion and Stress Evolution of Coal Pillar Failure Mechanism. *Rock Mech. Rock Eng.* **2022**, *55*, 2371–2383. [CrossRef]
14. Ran, Q.C.; Liang, Y.P.; Zou, Q.L.; Zhang, B.C.; Li, R.F.; Chen, Z.H.; Ma, T.F.; Kong, F.J.; Liu, H. Characteristics of Mining-Induced Fractures Under Inclined Coal Seam Group Multiple Mining and Implications for Gas Migration. *Nat. Resour. Res.* **2023**, *32*, 1481–1501. [CrossRef]

15. Wang, Q.; Gao, H.K.; Jiang, B.; Li, S.C.; He, M.C.; Wang, D.C.; Lu, W.; Qin, Q.; Gao, S.; Yu, H.C. Research on reasonable coal pillar width of roadway driven along goaf in deep mine. *Arab. J. Geosci.* **2017**, *10*, 466. [CrossRef]
16. Zhao, J.; Liu, C.Y.; Li, J.W.; Wang, W.C. Three-dimensional geological modeling and surface damage in gully area due to shallow coal seam mining. *J. Min. Saf. Eng.* **2018**, *35*, 969–977.
17. Wang, Q.W.; Feng, H.; Tang, P.; Peng, Y.T.; Li, C.A.; Jiang, L.S.; Mitri, H.S. Influence of Yield Pillar Width on Coal Mine Roadway Stability in Western China: A Case Study. *Processes* **2022**, *10*, 251. [CrossRef]
18. Shan, C.H.; Cao, S.G.; Zhang, Z.Y.; Lin, K.W.; Sun, J.L. Numerical Investigation on the Yield Pillar Bearing Capacity under the Two-End-Type Cable Reinforcement. *Energies* **2023**, *16*, 6418. [CrossRef]
19. Liang, T.; Liu, X.L.; Wang, S.J.; Wang, E.Z.; Li, Q.S. Study on the Fractal Characteristics of Fracture Network Evolution Induced by Mining. *Adv. Civ. Eng.* **2018**, *1*, 9589364. [CrossRef]
20. Miao, K.J.; Tu, S.H.; Tu, H.S.; Liu, X.; Li, W.L.; Zhao, H.B.; Tang, L.; Ma, J.Y.; Li, Y. Research on Fractal Evolution Characteristics and Safe Mining Technology of Overburden Fissures under Gully Water Body. *Fractal Fract.* **2022**, *6*, 486. [CrossRef]
21. Zhang, G.Z.; Guo, J.Z.; Xu, B.; Xu, L.L.; Dai, Z.X.; Yin, S.X.; Soltanian, M.R. Quantitative analysis and evaluation of coal mine geological structures based on fractal theory. *Energies* **2021**, *14*, 1925. [CrossRef]
22. Liu, C.; Xue, J.H.; Yu, G.F.; Cheng, X.Y. Fractal characterization for the mining crack evolution process of overlying strata based on microseismic monitoring technology. *Int. J. Min. Sci. Technol.* **2016**, *26*, 295–299. [CrossRef]
23. Zhang, Z.X.; Zhang, Y.B.; Xu, Y.X.; Zheng, Q.; Wang, Z.L.; Guo, L.L. Fracture development and fractal characteristics of overburden rock under repeated mining. *Arab. J. Geosci.* **2021**, *14*, 225. [CrossRef]
24. Han, P.H.; Zhang, C.; Wang, W. Failure analysis of coal pillars and gateroads in longwall faces under the mining-water invasion coupling effect. *Eng. Fail. Anal.* **2022**, *131*, 105912. [CrossRef]
25. Wang, P.; Luan, H.J. Size effect analysis of remaining coal pillar on rock burst caused by fault. *Bull. Eng. Geol. Environ.* **2022**, *81*, 1. [CrossRef]
26. Li, W.L.; Tu, S.H.; Tu, H.S.; Li, Y.; Liu, X.; Miao, K.J. Failure characteristics and control techniques for mining roadway affected by stress accumulation of residual pillars in contiguous coal seams. *Eng. Fail. Anal.* **2022**, *141*, 106646. [CrossRef]
27. Yang, P.J.; Zhang, S.R.; Wang, X.F. Numerical Study on the Characteristics and Control Method of Coal Leakage between Supports in Integrated Mining of Extremely Loose and Soft Coal Seams. *Energies* **2024**, *17*, 1013. [CrossRef]
28. Fan, N.; Wang, J.R.; Zhang, B.; Liu, D.; Wang, R.D. Reasonable Width of Segment Pillar of Fully-Mechanized Caving Face in Inclined Extra-Thick Coal Seam. *Geotech. Geol. Eng.* **2020**, *38*, 4189–4200. [CrossRef]
29. Ran, Q.C.; Chen, P.; Liang, Y.P.; Ye, C.F.; Zhang, B.C.; Wu, Z.P.; Ma, T.F.; Chen, Z.H. Hardening-damage evolutionary mechanism of sandstone under multi-level cyclic loading. *Eng. Fract. Mech.* **2024**, *307*, 110291.
30. Zhu, D.F.; Yu, B.B.; Wang, D.Y.; Zhang, Y.J. Fusion of finite element and machine learning methods to predict rock shear strength parameters. *J. Geophys. Eng.* **2024**, gxae064. [CrossRef]
31. Hu, J.H.; Ren, Q.F.; Yang, D.J.; Ma, S.W.; Shang, J.L.; Ding, X.T.; Luo, Z.Q. Cross-scale characteristics of backfill material using NMR and fractal theory. *Trans. Nonferrous Met. Soc. China* **2020**, *30*, 1347–1363. [CrossRef]
32. Hou, S.S.; He, X.; Meng, X.S.; Cheng, L.; Feng, Z.; Liu, M.X.; Li, A.; Guo, C.B.; Ji, F. Mesostructure and strength characteristics of granite under freeze-thaw cycles based on CT scanning. *J. Geomech.* **2024**, *30*, 462–472.
33. Zhang, G.C.; He, F.L.; Jia, H.G.; Lai, Y.H. Analysis of Gateroad Stability in Relation to Yield Pillar Size: A Case Study. *Rock Mech. Rock Eng.* **2017**, *50*, 1263–1278. [CrossRef]
34. Yang, P.J.; Zhang, S.R.; Liu, C.Y. Study on Shear Failure Process and Zonal Disintegration Mechanism of Roadway under High Ground Stress: A Numerical Simulation via a Strain-Softening Plastic Model and the Discrete Element Method. *Appl. Sci.* **2024**, *14*, 4106. [CrossRef]
35. Yu, B.; Zhang, Z.Y.; Kuang, T.J.; Liu, J.R. Stress Changes and Deformation Monitoring of Longwall Coal Pillars Located in Weak Ground. *Rock Mech. Rock Eng.* **2016**, *49*, 3293–3305. [CrossRef]